*31st EPS Conference on Plasma Phys. London, 28 June - 2 July 2004 ECA Vol.**28G**, P-1.153 (2004)*

Predictive modelling of electron temperature modulation experiments in JET L- and H-mode plasmas

P. Mantica[1], T.Tala[2], F. Imbeaux[3], M.Nora[4], V.Parail[5], J.Weiland[6] and the JET EFDA contributors

1. Istituto di Fisica del Plasma, EURATOM-ENEA-CNR Association, Milan, Italy
2. Association Euratom-Tekes, VTT Processes, PO Box 1608, Finland
3. CEA Cadarache, Association Euratom-CEA, S[t] Paul-lez-Durance Cedex, France
4. Helsinki Univ. of Technology, Association Euratom-Tekes, P.O.Box 2200, Finland
5. Culham Science Centre, Euratom/UKAEA Fusion Association, Abingdon, Oxon, UK
6. Chalmers Univ. of Technology and EURATOM-VR Assoc, S-41296 Göteborg, Sweden.

Power modulation experiments are a well known tool to investigate electron heat transport and provide additional insight into transport mechanisms with respect to steady-state analysis alone. The information provided by the dynamic plasma response to power perturbations constitutes a more discriminating experimental check of the performance of various different transport models than steady-state profile modelling, for which several different models can provide comparable results.

The present modelling work makes use of an experimental data base of JET discharges in L- and H-modes at low density (n_{e0}~$3\cdot10^{19}m^{-3}$) in which electron temperature (T_e) modulation experiments were performed using ICRH modulated power in mode conversion scheme [1,2]. Mode conversion takes place in D plasmas in the presence of a concentration of ~18% of ^{3}He (B_T~3.45 T, f_{ICRH}=33-37 MHz) and provides localized power deposition directly on electrons [3]. The power was square wave modulated with a frequency f_{mod}=15-20 Hz and duty-cycle 50%. The resulting T_e periodic perturbation was analysed with FFT techniques to extract profiles at the first 3 harmonics of amplitudes and cross-phases with respect to the power waveform. This set of data together with the steady-state profiles was used to test the results of fully predictive modelling, as described below.

The aim of the experiments was to explore the dependence of electron stiffness on the repartition of heating between the electron and ion channels [2]. It was found that plasmas with pure electron heating have mild electron stiffness, but applying ion heating causes a remarkable increase in electron stiffness. This is illustrated in Fig.1, where the amount of electron stiffness is plotted as a function of the ion temperature inverse gradient length R/L_{Ti} ($1/L_{Ti}=-\nabla T_i/T_i$) calculated in the region ρ=0.4-0.6. The amount of electron stiffness for each shot is obtained by fitting the modulation data using the ASTRA code with an empirical critical gradient model (CGM) for χ_e, as described in detail in [4]:

$$\chi_e = \chi_s q^{1.5} \frac{T_e}{eB}\frac{\rho_s}{R}\left(\frac{-R\nabla T_e}{T_e} - \kappa_c\right)H\left(\frac{-R\nabla T_e}{T_e} - \kappa_c\right) + \chi_0 q^{1.5}\frac{T_e}{eB}\frac{\rho_s}{R} \qquad (1)$$

Here $\rho_s=\sqrt{m_i T_e}/eB$, q is the safety factor, χ_0 and χ_s are dimensionless numbers giving respectively the residual and turbulent transport assuming a gyro-Bohm normalization, κ_c is the threshold. χ_0, χ_s and κ_c are the 3 free parameters (assumed constant in space and time) to be determined by best-fitting the data. In particular χ_s is the parameter providing an estimate of the level of stiffness. This determination is done by solving only the T_e and J equation, and assigning to n_e and T_i their experimental profiles. In the following the results of the best-fitted simulation with the empirical CGM model will be used as a reference for comparison with the results obtained by predictive modelling using widely used models.

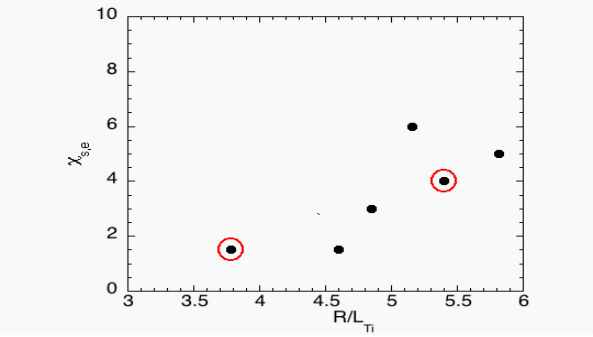

Fig.1: Experimentally determined trend of the amount of electron stiffness versus the ion temperature inverse gradient length. The two encircled shots are the ones chosen for the detailed predictive modelling with various transport models.

Amongst the available shots shown in Fig.1, two L-mode cases have been selected for the detailed predictive modelling, one (53822) representative of the pure (ICRH-MC) electron heating case and one (55809) representative of the case with the addition of strong NBI heating (9 MW). In the latter case the ITG instability is dominant, while in shots with pure electron heating the TEM instability has growing importance. One can see that the value of R/L_{Ti} increases from 3.8 to 5.4, which determines an increase of electron stiffness from χ_s~1.8 to χ_s~4. We note here that adding NBI heating also provides additional electron heating and therefore an increase of profile stiffness due to the factor $T_e^{3/2}$ in Eq.1. Our definition of stiffness however separates this effect from the intrinsic stiffness level expressed in the χ_s coefficient. It has been found by comparing L- and H-modes and shots with different amounts of ion and electron heating that in the experiment it is indeed the value of R/L_{Ti} that matters, rather than the absolute value of T_i or of the ratio T_e/T_i, as was originally proposed in [2].

The predictive modelling was performed solving all transport equations for T_e, T_i, n_e, J. The models under test were the Weiland model [5] (either collisionless or with collisions and electromagnetic effects included) and the Bohm-gyroBohm model [6], implemented in the transport code JETTO; the GLF23 model [7] version 1.61, implemented in the transport code ASTRA. Fig.2 shows for the pure electron heated discharge 53822 the predicted steady-state T_e, T_i and n_e profiles with the 3 models: Weiland collisional, Bohm-gyroBohm and GLF23. The same is shown in Fig.3 for shot 55809 with additional NBI heating. The Weiland collisionless model has been discarded because it fails to predict particle transport correctly. In fact it predicts far too peaked n_e profiles, which prevents a correct evaluation of the heat transport results in a fully predictive approach: it is found by forcing n_e to its experimental profile that the density peaking affects the amplitude and phase simulations, in the sense that a peaked n_e profile increases the amount of electron stiffness in the simulation, leading to a match of the experimental level of stiffness that is artificially induced by having a wrong n_e profile. From Fig.2 one can see how the 3 models considered match the steady-state profiles. It is evident that GLF and to a lesser extent Weiland overestimate T_i in the case of 53822. However this does not prevent further analysis of modulation data since it has been checked by forcing the absolute T_i value (but keeping R/L_{Ti} constant) that this does not affect the amount of electron stiffness. The use of GLF with predictive density has turned out to be very cumbersome. The model is very unstable and prone to crashes for both shots, but especially 53822. For 55809 it yields to the formation of an internal transport barrier in the density profile, which is not seen in experiment. Therefore the simulations with GLF23 shown here have been made by fixing the density profile close to experiment. This should not hinder the predictions of the model for heat transport since it is expected that for the R/L_n values of these shots (R/L_n~2.2 and R/L_n~1 respectively for 53822 and 55809) the density gradient should not contribute significantly to heat transport.

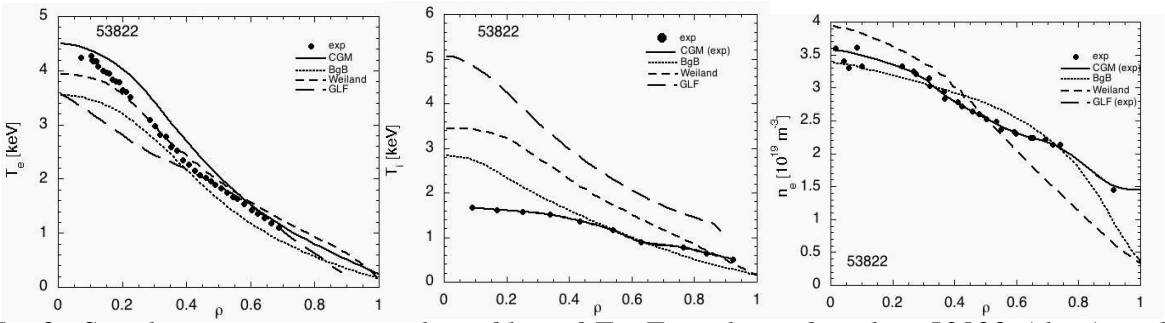

Fig.2: Steady-state experimental profiles of T_e, T_i and n_e for shot 53822 (dots) and simulations using various models: : empirical CGM (——), Weiland with collisions (– – –), Bohm-gyroBohm (.....) and GLF23(— —).

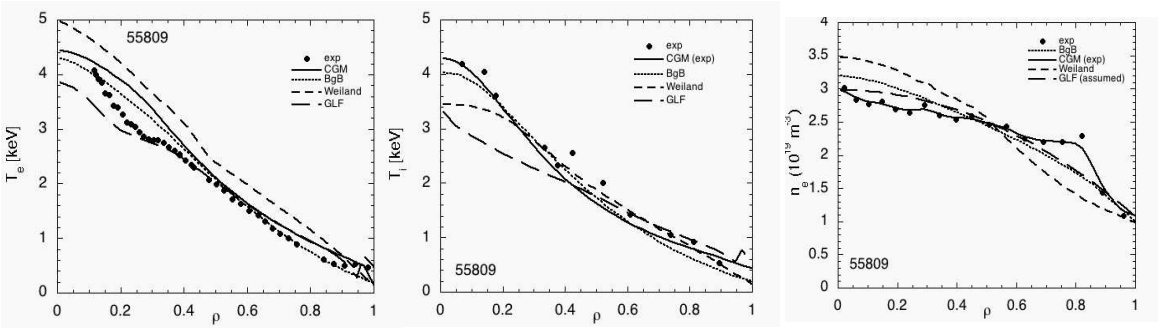

Fig.3: Steady-state experimental profiles of T_e, T_i and n_e for shot 55809 (dots) and simulations using various models: : empirical CGM (——), Weiland with collisions (– – –), Bohm-gyroBohm (.....) and GLF23(— —).

The performance of the various models in reproducing the modulation amplitude and phase profiles is illustrated in Figs.4 and 5. The empirical CGM simulation indicates a marked increase of electron stiffness from shot 53822 to shot 55809, correlated with the increase of R/L_{Ti}. As one can see from Figs.4 and 5, the best performing model appears to be the collisional Weiland model, which reproduces reasonably well the modulation data, although the 3rd harmonic is highly noisy. In particular the simulation of shot 53822 is very good, but for shot 55809 the model, although reproducing the experimental trend of

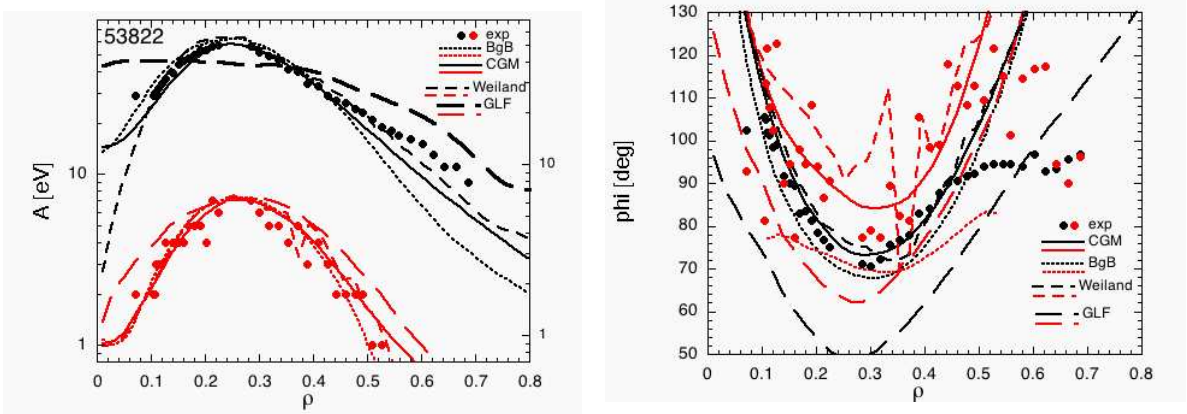

Fig.4: Experimental profiles (dots) of amplitude and phase at 1st (black) and 3rd (red) harmonic for shot 53822 and simulations using various models: empirical CGM (——), Weiland with collisions (– – –), Bohm-gyroBohm (.....) and GLF23(— —).

increasing stiffness with R/L_{Ti}, still underestimates the level of stiffness compared to experiment. The Bohm-gyroBohm model reproduces particularly badly the phase profiles,

in particular it does not provide the usual diffusive scaling of the phase minimum value with frequency. GLF23 performs very badly for shot 53822, whereas is comparable to the Weiland model for shot 55809.

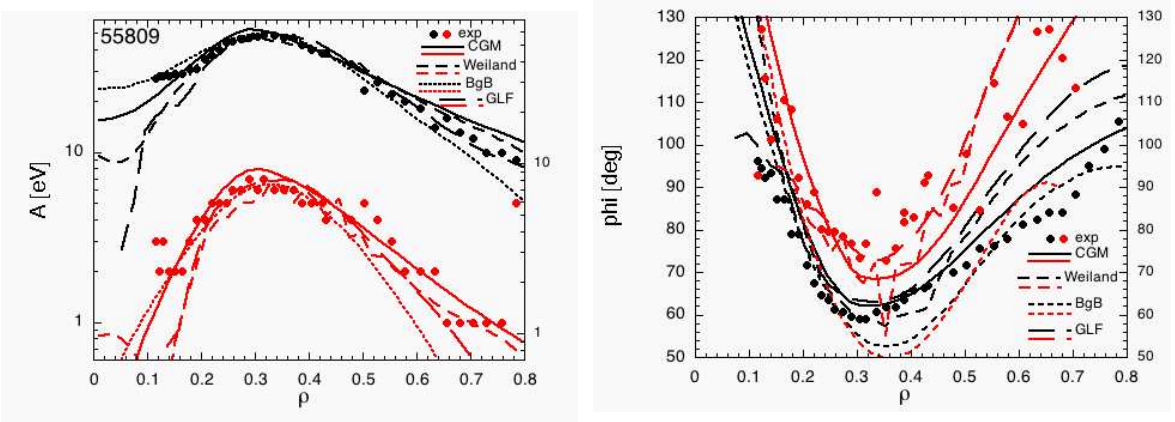

Fig.5: Experimental profiles (dots) of amplitude and phase at 1st (black) and 3rd (red) harmonic for shot 55809 and simulations using various models: empirical CGM (___), Weiland with collisions (– – –), Bohm-gyroBohm (·····) and GLF23 (— — —).

In order to investigate further the role of R/L_{Ti} on electron stiffness in the Weiland model, we have varied the NBI power arbitrarily starting from the simulations of Figs.4 and 5, in order to induce a variation of R/L_{Ti}, and study the change in amplitude and phase slopes (we remind that flatter amplitudes and phases mean larger perturbative χ and therefore stronger stiffness). Fig.6 for example shows that starting from shot 53822 and increasing the value of R/L_{Ti} the electron stiffness is indeed increased. In fact the changes in A and φ slopes imply an increase of perturbative χ of about a factor 2. T_e is only changing by 15%, so the increase of stiffness is mainly attributed to the change in R/L_{Ti}.

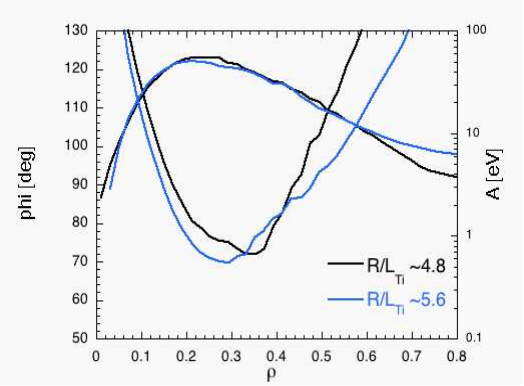

Fig.6: Simulations using Weiland model at two different values of R/L_{Ti}, starting from the simulation of shot 53822 shown in Fig.4 (black) and increasing R/L_{Ti} (cyan).

In conclusion, 3 widely used transport models (Weiland collisional, GLF23 and Bohm-gyroBohm) have been tested against modulated T_e experiments in JET discharges with electron stiffness strength varying in correlation with ion heating (R/L_{Ti}). The Weiland collisional model was found the one most reasonably reproducing the experimental data.

We thank X.Garbet, F.Ryter and C.Angioni for precious discussions.

[1] P.Mantica et al., Transient Heat Transport Studies in JET Conventional and Advanced Tokamak Plasmas, in Fusion Energy 2002 (Proc. 19th IAEA Conf. Lyon, 2002), EX/P1-04, IAEA (2002).
[2] P.Mantica et al., Heat wave propagation experiments and modelling at JET: L-mode, H-mode and ITBs, in Controlled Fusion and Plasma Physics (Proc. 30th Eur. Conf. St..Petersburg, 2003), O-3.1A, EPS (2003).
[3] M.Mantsinen et al., Nuclear Fusion 44 (2004) 33.
[4] X.Garbet et al., "Profile stiffness and global confinement", accepted for publication in Plasma Phys. Control. Fusion.
[5]] J. Weiland , "Collective modes in inhomogeneous plasma", Kinetic and Advanced Fluid Theory, IoP Publishing, Bristol and Philadelphia 2000.
[6] M.Erba et al., Plasma Phys. Control. Fusion 39 (1997) 261.
[7] R.E.Waltz et al., Phys.Plasmas 4 (1997) 2482.